Development 140, 3146-3155 (2013) doi:10.1242/dev.093682

Apical constriction initiates new bud formation during monopodial branching of the embryonic chicken lung

Hye Young Kim[1,*], Victor D. Varner[1,*] and Celeste M. Nelson[1,2,‡]

SUMMARY

Branching morphogenesis sculpts the airway epithelium of the lung into a tree-like structure to conduct air and promote gas exchange after birth. In the avian lung, a series of buds emerges from the dorsal surface of the primary bronchus via monopodial branching to form the conducting airways; anatomically, these buds are similar to those formed by domain branching in the mammalian lung. Here, we show that monopodial branching is initiated by apical constriction of the airway epithelium, and not by differential cell proliferation, using computational modeling and quantitative imaging of embryonic chicken lung explants. Both filamentous actin and phosphorylated myosin light chain were enriched at the apical surface of the airway epithelium during monopodial branching. Consistently, inhibiting actomyosin contractility prevented apical constriction and blocked branch initiation. Although cell proliferation was enhanced along the dorsal and ventral aspects of the primary bronchus, especially before branch formation, inhibiting proliferation had no effect on the initiation of branches. To test whether the physical forces from apical constriction alone are sufficient to drive the formation of new buds, we constructed a nonlinear, three-dimensional finite element model of the airway epithelium and used it to simulate apical constriction and proliferation in the primary bronchus. Our results suggest that, consistent with the experimental results, apical constriction is sufficient to drive the early stages of monopodial branching whereas cell proliferation is dispensable. We propose that initial folding of the airway epithelium is driven primarily by apical constriction during monopodial branching of the avian lung.

KEY WORDS: Morphodynamics, Patterning, Mechanical stress, Biomechanics

INTRODUCTION

The intricate network of branched airways of the lung originates as a simple epithelial tube. A sequence of recursive branching events then transforms this simple tubular geometry into a complex system of airways that conduct air and promote gas exchange postnatally. In the early chicken embryo, this process is monopodial; that is, daughter branches emerge laterally along the length of their parent branch (Locy and Larsell, 1916; Hogan, 1999). This branching strategy generates a structure distinct from that in the mammalian lung, which is formed instead by a combination of lateral and dichotomous branching modes (Metzger et al., 2008). Moreover, because airflow is unidirectional in the lungs of birds, as opposed to tidal in mammals, some of these monopodial branches anastomose to form circulatory loops called air capillaries. Other branches dilate at their distal tips to form large air sacs, which then function like bellows to maintain a constant unidirectional flow.

These dramatically different architectures suggest distinct underlying developmental mechanisms. Yet, remarkably, several signaling pathways, including those downstream of fibroblast growth factor (FGF), bone morphogenetic protein (BMP) and sonic hedgehog (SHH), are conserved across different species and different organ systems (Metzger and Krasnow, 1999; Affolter et al., 2003; Morrisey and Hogan, 2010). This molecular homology underlies the hypothesis that the physical mechanisms that sculpt these branching structures are likewise conserved (Hogan, 1999; Davies, 2002). Branching of many organs is thought to result from local increases in proliferation along the epithelium (Goldin and Wessells, 1979; Goldin and Opperman, 1980; Moore et al., 2002; Moore et al., 2005; Morrisey and Hogan, 2010), but unambiguous experimental evidence for this mechanism is lacking (Wessells, 1970; Nogawa et al., 1998). Whether patterned proliferation is sufficient to generate the observed deformations remains unclear. Recent studies, however, have suggested a possible regulatory role for mechanical forces and cytoskeletal contractility during branching (Michael et al., 2005; Moore et al., 2005; Nelson and Gleghorn, 2012). Quantitative studies focused on the mechanics of branching (Caussinus et al., 2008; Gjorevski and Nelson, 2010) are therefore required to define the physical forces that shape the developing airways.

Here, we examined the relative roles of actomyosin contraction and cell proliferation in the initiation and outgrowth of buds during monopodial branching of the embryonic chicken lung. Combining quantitative image analysis with computational modeling, we found that apical constriction of the airway epithelium is sufficient to drive the changes in cell and tissue shape required for initial budding during monopodial branching. Moreover, we also found a complex pattern of proliferation along the primary bronchus, enriched along the dorsal and ventral aspects of the tube and highest in regions prior to branching. Nonetheless, both experiments and simulations revealed that proliferation, coupled with the forces generated by apical constriction, was not sufficient to fully shape the emerging lung bud. These results challenge the generally accepted view that patterned proliferation drives airway branching morphogenesis, and suggest instead that active shape changes of the epithelium play a major role in the branching process.

MATERIALS AND METHODS

Ex vivo culture of embryonic chicken lungs

Fertilized chicken eggs were obtained from a commercial vendor (Hyline) and incubated in a rotating incubator (GQF Manufacturing Company) maintained at 37°C and 60% humidity until the desired stage. Embryonic

[1]Department of Chemical and Biological Engineering, Princeton University, Princeton, NJ 08544, USA. [2]Department of Molecular Biology, Princeton University, Princeton, NJ 08544, USA.

*These authors contributed equally to this work
‡Author for correspondence (celesten@princeton.edu)

Accepted 14 May 2013

lungs were dissected using a pair of forceps in cold PBS supplemented with antibiotics (50 units/ml of penicillin and streptomycin; Invitrogen). Dissected lungs were cultured over a porous membrane (nucleopore polycarbonate track-etch membrane, 8 μm, 25 mm; Whatman) in DMEM/F12 medium (without HEPES) supplemented with 5% fetal bovine serum (FBS, heat inactivated; Atlanta Biologicals) and antibiotics (50 units/ml each of penicillin and streptomycin) (Miura et al., 2009; Gleghorn et al., 2012). To alter the rate of proliferation, we varied the concentration of FBS in the culture medium; these treatments had no effect on the relative pattern of proliferation. The pharmacological inhibitors aphidicolin (Sigma), blebbistatin (Sigma) and SU5402 (Santa Cruz) were added to the culture medium and the phenotype of the lung explants was monitored under brightfield illumination on an inverted microscope (Nikon Ti) using a 2× objective.

Immunofluorescence staining and imaging

In general, dissected lungs were fixed with 4% paraformaldehyde in PBS for 15 minutes at room temperature. For staining of F-actin, 0.25% glutaraldehyde was added to the fixative. For staining of α-tubulin, we used ice-cold Dent's fixative (1:4 ratio of DMSO:methanol). Fixed lungs were washed with 0.3% Triton-X-100 in PBS and blocked with 10% goat serum. The following primary antibodies were used: anti-pMLC-2 (Ser19, Cell Signaling), anti-LCAM (7D6, Developmental Studies Hybridoma Bank), anti-β-catenin (Sigma), anti-α-tubulin (Sigma) and anti-cleaved caspase-3 (Cell Signaling). After extensive washing, samples were incubated in Alexa Fluor-conjugated secondary antibody or phalloidin (Invitrogen). Proliferating cells were detected using the Click-iT EdU Imaging Kit (Invitrogen). As a positive control for apoptosis, lungs were treated with staurosporine (1 μM; Cell Signaling) prior to fixation. Stained lungs were dehydrated in a methanol series and optically cleared with Murray's clear (1:2 ratio of benzyl alcohol:benzyl benzoate; Sigma) for confocal imaging. Confocal stacks were collected using a spinning disk confocal (BioRad) fitted to an inverted microscope and analyzed using ImageJ (Schneider et al., 2012).

Theoretical methods

To simulate lung bud formation, we constructed a three-dimensional (3D) nonlinear finite element model of the primary bronchial tube in COMSOL Multiphysics (Version 4.2a; Burlington, MA, USA) (Fig. 3). As discussed below, each bud showed a similar pattern of actomyosin staining and formed as a repeated structure along the tube. We therefore modeled an individual bud and assumed it to be representative of all buds emerging from the primary bronchus.

The bronchial tube was modeled as a thick-walled, hollow cylinder of length L and thickness $t = R_o - R_i$, where R_o and R_i represent the outer and inner radii of the tube, respectively (Fig. 3A). Regions of apical constriction were specified on the dorsal and ventral sides of the tube, bounded by either the angle α or the angle β as well as the length, L_{bud}. These regions did not undergo apical constriction homogeneously. Rather, gradients in apical constriction were specified based on experimentally observed patterns of F-actin staining (supplementary material Fig. S1). In addition, a plane of symmetry was assumed through the mid-plane of the bud (Fig. 3A).

We used a theory for finite volumetric growth to model both apical constriction and cell proliferation in the lung epithelium (Rodriguez et al., 1994). Briefly, active shape changes in the tissue were simulated by decomposing the overall deformation gradient tensor $\mathbf{F}$ into a component due to growth (or contraction) and a component due to elastic deformation by $\mathbf{F} = \mathbf{F}^* \cdot \mathbf{G}$, where $\mathbf{G}$ is the growth tensor and $\mathbf{F}^*$ is the elastic deformation gradient tensor. This framework has been used previously to model both cardiac c-looping (Voronov et al., 2004) and head fold formation (Varner et al., 2010) in the chicken embryo, and ventral furrow formation (Muñoz et al., 2007; Muñoz et al., 2010) in *Drosophila*.

The growth tensor $\mathbf{G}$ was then further decomposed into a component due to apical constriction $\mathbf{G}_1$ and a component due to cell proliferation $\mathbf{G}_2$ by $\mathbf{G} = \mathbf{G}_2 \cdot \mathbf{G}_1$. To simulate apical constriction, cuboidal elements in the bud-forming region acquired wedge-shaped geometries by constricting isotropically (in the θ and z directions) at their apices and expanding isotropically (in the θ and z directions) at their bases (Fig. 3A). The amount of wedging was specified by the components of $\mathbf{G}_1$, which were referred to the cylindrical set of basis vectors $\mathbf{e}_r$, $\mathbf{e}_\theta$, $\mathbf{e}_z$, such that:

$$\mathbf{G}_1 = \mathbf{e}_r\mathbf{e}_r + G_1\mathbf{e}_\theta\mathbf{e}_\theta + G_1\mathbf{e}_z\mathbf{e}_z \,, \tag{1}$$

and

$$G_1 = 1 + dG_i + \frac{R - R_i}{R_o - R_i}\left(dG_o - dG_i\right), \tag{2}$$

where dG_i and dG_o are the growth stretch ratios along the inner and outer surfaces of the tube, respectively, and R_i and R_o are the inner and outer radii of the un-deformed epithelial tube, respectively. Here, we considered $dG_i = -dG_o$, such that shortening along the apical side of the epithelium produced a compensatory lengthening along the basal side to ensure that cell volume was approximately conserved.

Cell proliferation both within and adjacent to the bud-forming region was specified by:

$$\mathbf{G}_2 = \mathbf{e}_r\mathbf{e}_r + G_\theta\mathbf{e}_\theta\mathbf{e}_\theta + G_z\mathbf{e}_z\mathbf{e}_z \,, \tag{3}$$

where G_θ and G_z represent the amounts of proliferation oriented along the θ and z directions, respectively. Details for implementing this framework in COMSOL can be found in a previous publication by Taber (Taber, 2008).

As a first approximation, we assumed a pseudoelastic constitutive response for the tissue and considered the following Blatz-Ko strain energy density function:

$$W = C\left(I_1^* - 3 + \frac{1-2\nu}{\nu}\left(J^{*-2\nu/(1-2\nu)} - 1\right)\right), \tag{4}$$

where C and ν are material constants, I_1^* is the modified first invariant of the right Cauchy-Green elastic deformation gradient tensor $\mathbf{C}^* = \mathbf{F}^{*T} \cdot \mathbf{F}^*$, and J^* is the elastic dilatation ratio. For small strains, ν represents Poisson's ratio, but has no physical meaning for problems involving large deformations (Taber, 2004). In all simulations, we assumed slight material compressibility $\eta = 0.45$. To simulate tissue stiffening during apical constriction, C was increased (relative to the stiffness of the tissue in passive regions, C_p) in regions of the tissue actively undergoing shape changes.

The Cauchy stress tensor $\boldsymbol{\sigma}$, which depends only on the elastic component of the deformation $\mathbf{F}^*$, was then computed by (Taber, 2004):

$$\boldsymbol{\sigma} = J^{*-1}\mathbf{F}^* \cdot \frac{\partial W}{\partial \mathbf{F}^{*T}} \,, \tag{5}$$

Image analysis and statistics

Quantitative analysis and projection of confocal images were carried out using ImageJ (Schneider et al., 2012). To quantify proliferating epithelial cells, we first collected confocal stacks of double-stained (LCAM and EdU) lung explants for stages with one to three buds (b1 to b3). Cross-sectional images were reconstructed (Fig. 5B) along the length of the bronchus, and EdU-positive cells within the epithelium were counted approximately every 10 μm along the bronchus (proximal, bud, distal). We counted the proliferating cells in the first bud region (b1) across all stages (one to three buds). To quantify apical constriction, we assumed that morphological differences between multiple buds at an individual stage of development were representative of dynamic changes in an individual bud over time. Quantitative analysis of cell geometries was performed on cells spanning the full thickness of the epithelium within buds b1-b3 in fixed explants at Hamburger and Hamilton (HH) stage 26. Statistical significance was calculated using IBM SPSS statistics 19 (IBM) using the *t*-test for changes in number of buds and ANOVA for comparisons of different stages and treatments.

RESULTS

Apical constriction of the airway epithelium initiates budding from the primary bronchus

The airway epithelium of the embryonic chicken lung undergoes monopodial branching morphogenesis, which consists of initiation of budding from the primary bronchus followed by bud outgrowth (Locy and Larsell, 1916). This monopodial branching is analogous to domain branching in the embryonic mouse lung, in which

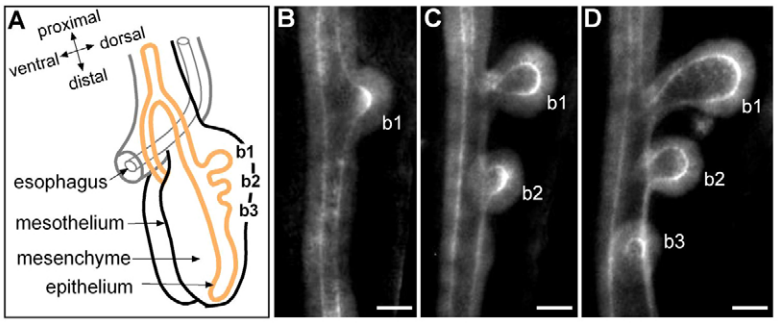

Fig. 1. Branching morphogenesis of the embryonic chicken lung. (**A**) Schematic of embryonic chicken lung at HH27. Lung epithelium (in orange) surrounded by mesenchyme undergoes monopodial branching, which occurs sequentially along the primary bronchus in a distal direction. (**B-D**) Airway epithelial branching morphogenesis shown in LCAM-stained embryonic chicken lung between HH25 (1-bud stage) and HH27 (3-bud stage). Maximum intensity of confocal sections for 20 μm-thick tissues is projected. The first lung bud (b1) emerges around HH25 (B) and the subsequent buds (b2 and b3) form within 24 hours (D). b, bud; HH, Hamburger-Hamilton stage. Scale bars: 50 μm.

daughter branches bud laterally off of the circumference of the parent branch (Metzger et al., 2008). In the embryonic chicken lung, the primary bronchus is a simple epithelial tube surrounded by a thick mesenchyme and an outer layer of mesothelium (Locy and Larsell, 1916). Monopodial budding of the bronchus begins at Hamburger-Hamilton (HH) stage 25 (Fig. 1), and the first three buds (b1-b3) emerge sequentially in a cranial-to-caudal direction over a 24-hour period at precise locations along the dorsal surface of the primary bronchus (Fig. 1B-D) (Gleghorn et al., 2012).

To characterize the cellular forces that operate during the branching process, we examined the role of actomyosin contraction in the epithelium of the primary bronchus. Lungs were stained for filamentous actin (F-actin) and phosphorylated myosin light chain (pMLC) and imaged by confocal microscopy. Three-dimensional (3D) reconstruction of confocal stacks revealed that F-actin was enriched at the apical surface of the emerging bud epithelium (Fig. 2A; supplementary material Movie 1), and colocalized with pMLC (Fig. 2B). These data suggested that the apical surface of the dorsal airway epithelium undergoes constriction during new bud formation. Surprisingly, we also observed enrichment of F-actin and pMLC at the apical surface of the non-budding epithelium on the ventral side of the bronchial tube (Fig. 2A, *yz* slice), which formed a figure-eight-shaped cross-section at the earliest stages of budding. Staining for the cell-cell adhesion protein LCAM (E-cadherin) (supplementary material Fig. S1E,F) revealed an increase in the density of intercellular adhesions at the apical surface of nascent buds. Quantitative analysis of cell geometries within buds at different stages of extension showed that the apical cross-sectional width decreased significantly (Fig. 2C-G), confirming constriction of the apical membrane during the budding process.

To determine whether apical constriction is required to fold the airway epithelium during monopodial budding, we selectively inhibited actomyosin contractility using the non-muscle myosin ATPase inhibitor blebbistatin (Straight et al., 2003; Kovács et al., 2004). Treating embryonic lung explants with blebbistatin (5 μM) significantly reduced the initiation of new buds over a 24-hour period of culture (Fig. 2H,I). Branching morphogenesis of the avian (Moura et al., 2011) and mammalian (Bellusci et al., 1997; Abler et al., 2009) lungs is regulated via signaling through FGF, which has also been shown to induce actomyosin contraction during morphogenesis of the inner ear (Sai and Ladher, 2008) and apical constriction of the rosettes that form the lateral line in zebrafish (Harding and Nechiporuk, 2012). Consistently, we found that treatment with an FGF receptor kinase inhibitor, SU5402 (5 μM), blocked apical constriction (supplementary material Fig. S2) and epithelial budding from the primary bronchi (Fig. 2H,J). These results suggest that apical constriction is one of the physical deformations required to initiate folding of the embryonic airway epithelium into a nascent bud during monopodial branching.

Apical constriction can only create the initial geometry of the bud

To examine whether the forces generated during apical constriction were by themselves sufficient to physically drive monopodial budding, we constructed a 3D model of the primary bronchus using the finite element method (FEM). As described in Materials and methods, we modeled the airway epithelium as a uniform, thick-walled cylinder (Fig. 3A). Active shape changes in the tissue were simulated using a continuum theory for finite volumetric growth (Rodriguez et al., 1994). Consistent with the accumulations of F-actin, pMLC and LCAM observed experimentally, apical constriction was specified in the bud-forming region of the primary bronchus (bounded by the angle α and length L_{bud}), as well as along the ventral aspect of the epithelial tube immediately opposite the forming bud (bounded by the angle β and length L_{bud}). In these regions, cuboidal elements in the tissue actively became wedge-shaped (Fig. 3A), and the amount of apical constriction was defined by specifying the components of the growth tensor $\mathbf{G}_1$. In longitudinal section, the average magnitude of G_1 along the apical surface was 0.49, which was consistent with our analysis of cell geometries (Fig. 2C,E). Moreover, because cells and tissues stiffen when they contract (Wakatsuki et al., 2000; Wakatsuki et al., 2001; Rémond et al., 2006; Zhou et al., 2009; Varner and Taber, 2012), we assumed that the cells undergoing apical constriction during bud formation exhibited a similar material stiffening.

When both apical constriction and the resulting tissue stiffening were included, the model produced a bud geometry similar to that observed experimentally during the initial stages of monopodial branching (compare Fig. 3B,C with Fig. 2A; supplementary material Movie 2). Somewhat surprisingly, the model also predicted the lemniscate (i.e. figure-eight-shaped) geometry of the cross-section of the bud (Fig. 3B), but only if tissue stiffening was included (Fig. 3D). For a given increase in stiffness, however, the extent to which the model was able to produce a lemniscate cross-section depended on the thickness of the tube (supplementary material Fig. S3); the thickness used in our model yielded the most physiologically realistic geometries (Fig. 3D). Still, even for thicker tubes, sufficiently large stiffening could be specified to form a lemniscate cross-section (unpublished data). Even so, our simulations suggested that, at most, apical constriction itself could only initiate the early stages of bud formation (Fig. 3D). On its own, apical constriction was unable to generate the more fully developed geometry of the bud (shown in longitudinal section in Fig. 1C,D), even though spatial gradients of the amount of specified apical constriction were similar qualitatively to the gradients of F-actin intensity measured experimentally (supplementary material Fig. S1).

The results of these simulations suggested that additional cellular behaviors are required to complete the formation of a monopodial

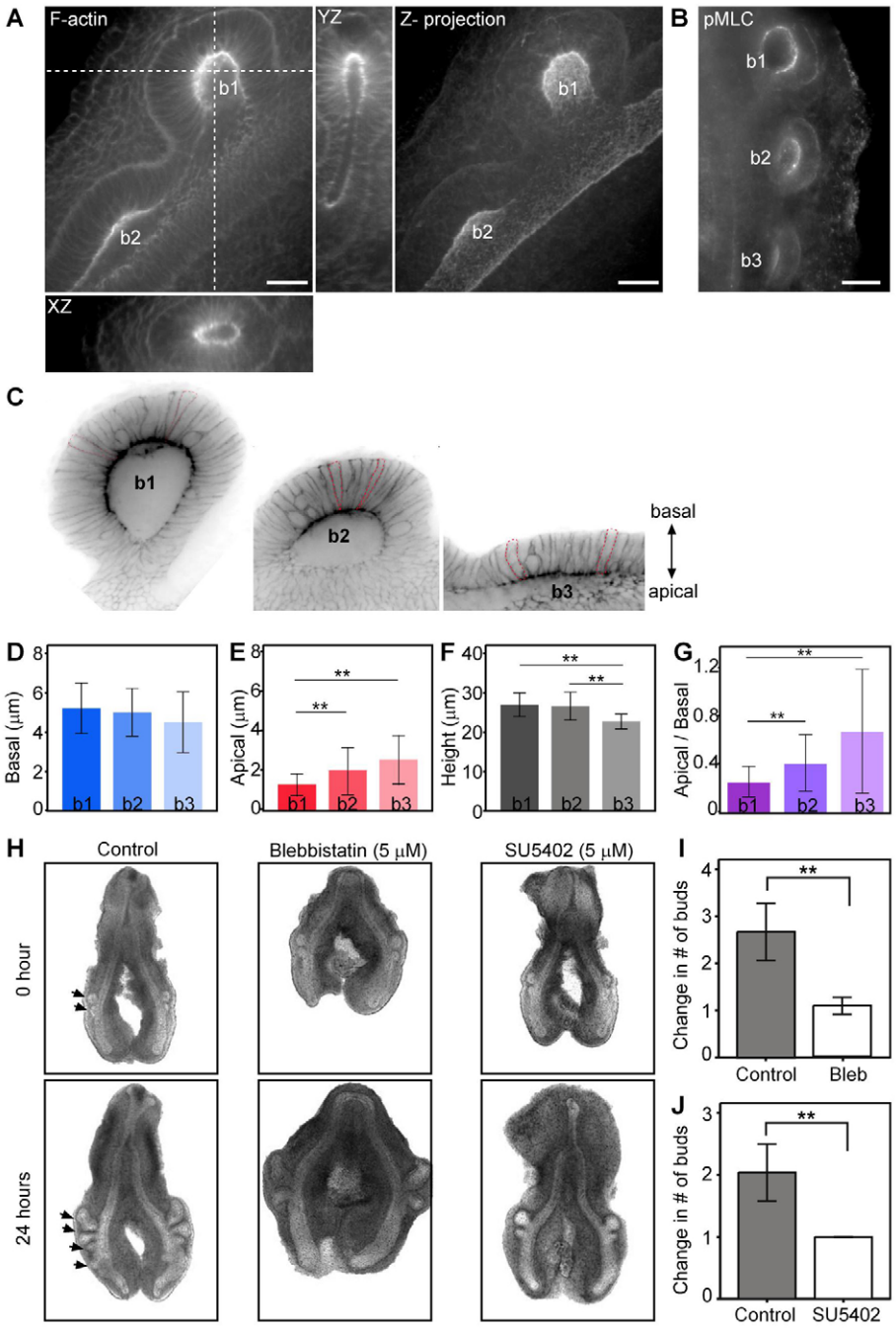

Fig. 2. Apical constriction initiates new bud formation. (**A**) Confocal sections of a phalloidin-stained lung at the 2-bud stage, showing strong F-actin localization in the apical domain of the epithelium in emerging buds (b1 and b2). Orthogonal views from white dashed lines show the cross-section of the emerging b1, revealing apical constriction also in the ventral epithelium and the resulting lemniscate geometry. The maximum intensity of confocal sections of 55 μm-thick tissues is projected. Scale bars: 20 μm. (**B**) High levels of pMLC are present at the apical surface of the lung buds. Maximum intensity of 25 μm-thick tissue section is presented. Scale bar: 50 μm. (**C-G**) Quantification of the cross-sectional dimensions of epithelial cells at different budding stages (n=122 from four lungs, $^{**}P$<0.01, error bars represent s.d.). Representative cells are outlined with red dotted lines in C. Average basal width (D), apical width (E) and cell height (F) were measured from confocal sections. (**H**) Brightfield images of explants cultured in the presence of blebbistatin (5 μM) or SU5402 (5 μM) for 24 hours. (**I**,**J**) Fold change in the number of buds after 24 hours of culture (n=9, $^{**}P$<0.01, error bars represent s.d.).

bud. As the lung epithelium has been shown to be highly proliferative, we next assessed whether accounting for cell proliferation might produce the more fully developed lung bud geometries observed experimentally.

Cell proliferation is not required for initiation of new buds

The developing chicken lung more than doubles in size during its first 24 hours of culture *ex vivo* (Gleghorn et al., 2012), as the majority of cells are proliferating during its morphogenesis (Fig. 4A). Differential cell proliferation has been proposed to be essential for bud formation during branching morphogenesis of the mammalian lung and kidney (Goldin et al., 1984; Nogawa et al., 1998; Moore et al., 2002; Michael and Davies, 2004; Moore et al., 2005), although proliferation is apparently not required for branching of the salivary gland (Nakanishi et al., 1987; Spooner et al., 1989). To test whether cell proliferation is necessary for monopodial branching of the avian lung, we blocked progression of the cell cycle using the DNA synthesis inhibitor aphidicolin. Despite complete inhibition of cell proliferation, which was evident after both 3 hours and 24 hours of treatment as visualized by staining for incorporation of the thymidine analog 5-ethynyl-2′-deoxyuridine (EdU) (Fig. 4A,B), the airway epithelium continued to form new buds (Fig. 4C,D). Aphidicolin-treated explants formed buds with essentially the same geometry as those from control explants, and high magnification images revealed that aphidicolin-treated buds comprised fewer but larger cells than control buds (supplementary material Fig. S4A). Consistently, increasing cell proliferation by treating with high concentrations of serum had no effect on monopodial budding (supplementary material Fig. S4B-E).

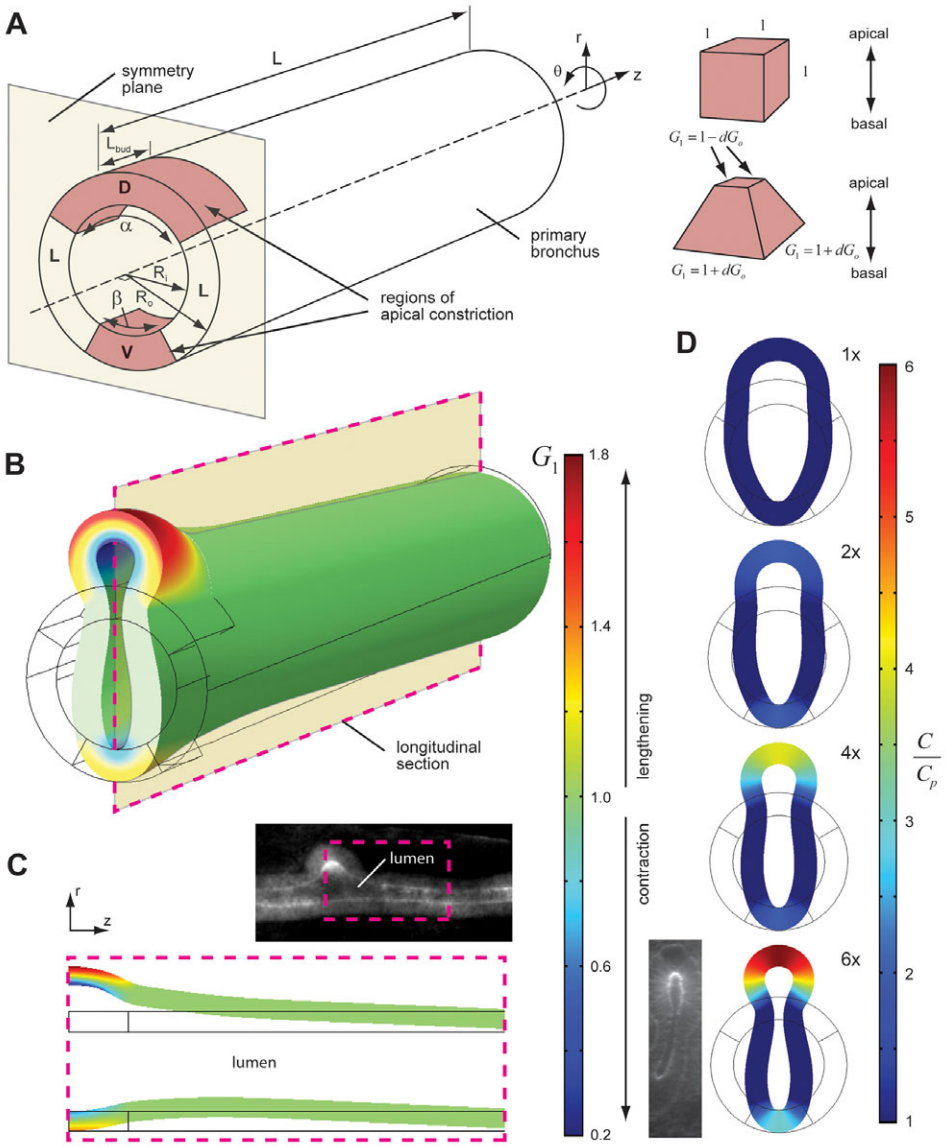

Fig. 3. Apical constriction (by itself) can only initiate early stages of bud formation. (**A**) Model schematic. The primary bronchus was modeled as a tube of length L and thickness $t = R_o - R_i$. Apical constriction was specified in a bud-forming region of the tube (bounded by the angle $\alpha = 120°$ and length L_{bud}), as well as along its ventral aspect (bounded by the angle $\beta = 60°$ and length L_{bud}). In these regions, cuboidal elements within the tissue became wedge-shaped (see inset). The amount of wedging was specified by the scalar G_1, which represents the θ and z components of the growth tensor $\mathbf{G}_1$. See text for details. D, dorsal; L, lateral; V, ventral. (**B**) Deformed model geometry. The magnitude of G_1 specifies the amount of apical constriction in the tissue; $G_1 > 1$ indicates an active lengthening, whereas $G_1 < 1$ indicates an active shortening. (**C**) Longitudinal section of model geometry (along plane specified in B). The model bud geometry qualitatively matches that observed experimentally (dashed box in inset). (**D**) Transverse sections of model geometry. To simulate tissue stiffening, the ratio C/C_p was increased in regions undergoing apical constriction, where C_p represents the passive material stiffness. As stiffening was increased from 1× to 6×, the model more closely matched the lemniscate cross-section of the bud.

These data suggest that cell proliferation is not required to initiate monopodial branching of the avian airway epithelium.

Combining proliferation with apical constriction is insufficient to fully shape the lung bud

Might cell proliferation play a role during bud outgrowth? To address this question, we quantified the proliferation of the branching airway epithelial cells along the primary bronchus, from stages with one bud to those with three buds. To simplify the analysis, we specified three regions along the primary bronchus: the proximal region, representing the non-budding epithelium; the bud region, representing the actively budding epithelium; and the distal region, representing the future budding epithelium (Fig. 5A,B). Although epithelial cells were proliferating along the entire length of the bronchus, we noted a significant increase in the number of proliferating cells in the distal region of the epithelium, suggesting that epithelial proliferation precedes bud formation (Fig. 5C). Furthermore, analysis of the spatial distribution of proliferating cells within the distal region indicated preferential epithelial growth along the dorsal and ventral sides of the primary bronchus (Fig. 5D). We found that within the epithelium of the bud region, proliferation was confined to the dorsal epithelial cells, which presumably participate in bud outgrowth (Fig. 5D). In the epithelium of the proximal region, the pattern of proliferation varied over time; at the 3-bud stage, the epithelium in this region was largely quiescent (Fig. 5D). We found little discernible apoptosis within the airway epithelium at these stages (supplementary material Fig. S5), consistent with previous reports (Moura et al., 2011).

We then included cell proliferation in our computational model to test whether the combination of proliferation and apical constriction could generate the more fully developed bud morphology observed in experiments (see b1 in Fig. 1C). Consistent with EdU staining in lungs containing one bud (Fig. 5), we modeled cell proliferation in the bud-forming region of the primary bronchus, as well as in the distal region of the tube (Fig. 6A); twice as much growth was included in this adjacent (i.e. distal) region (compare with Fig. 5C). Moreover, because cell proliferation was preferentially confined to the dorsal and ventral sides of the tube (Fig. 5D), we specified growth around the circumference that matched our experimental observations (Fig. 6A, insets).

Although our EdU results provided information about the overall magnitude of proliferation in the epithelium, these data did not

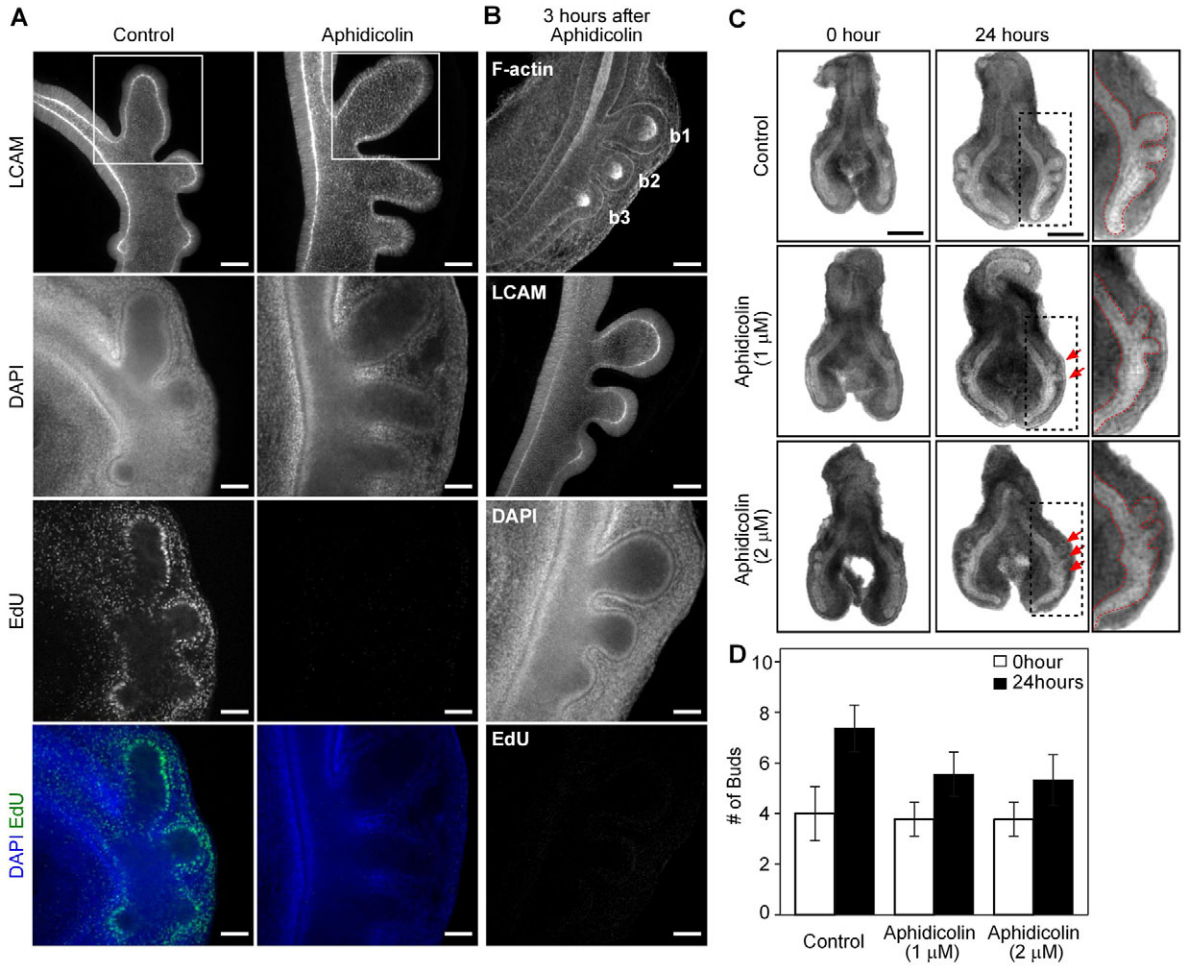

Fig. 4. Cell proliferation is not required to initiate new buds. Despite inhibiting cell proliferation, the airway epithelium continues to form new buds. (**A**,**B**) Staining for EdU incorporation at 24 hours (A) and 3 hours (B) after treatment with aphidicolin (1 μM) confirmed that proliferation was blocked. High-magnification views of the white inset areas are shown in supplementary material Fig. S4. Scale bars: 50 μm. (**C**) Brightfield images of embryonic chicken lung explants cultured in the presence of aphidicolin (red arrows indicate buds, high-magnification view of the black dashed inset areas shown on right). Scale bars: 500 μm. (**D**) Change in the number of buds after 24 hours of aphidicolin treatment (*n*=9, error bars represent s.d.).

indicate whether there was any preferential orientation or directionality. Our model enabled us to examine the relative effects of either oriented or isotropic (i.e. unoriented) growth on bud morphology (Fig. 6A). These patterns of cell division were superimposed on the distribution of apical constriction specified above (Fig. 6A′). We found that only when growth was oriented along the axial length of the tube did a neck-like region begin to form in the developing bud (Fig. 6B,C; supplementary material Movie 3). Specifying axial growth in the bud-region alone was insufficient to generate this bud geometry (supplementary material Fig. S6), thus indicating a possible morphogenetic role for proliferation in regions adjacent to the forming bud. Similarly, isotropic (Fig. 6D,E) and circumferential (Fig. 6F,G) growth merely produced a local distension of the tube and did not qualitatively affect the morphology of the bud.

Our computational model thus predicted that monopodial budding is accompanied by axially directed cell division within the distal region of the primary bronchus. To test these predictions experimentally, we stained lungs at various stages for β-catenin to define cell boundaries and α-tubulin to label the mitotic spindle. Quantitative analysis of spindle orientation within confocal stacks revealed that cells within the distal region divided preferentially along the axial length of the tube (supplementary material Fig. S7). Still, even in the case of axial growth, our computational model was unable to reproduce the more fully developed bud geometry (i.e. a more narrowed neck-region). These data suggest that although proliferation may contribute physically to the budding process, apical constriction and growth alone are insufficient to fully shape the early lung bud. Importantly, further simulations indicated that proliferation was not sufficient to initiate budding in the absence of apical constriction (supplementary material Fig. S8).

DISCUSSION

Branching morphogenesis of the lung requires reciprocal interactions between the airway epithelium and its surrounding mesenchyme (Metzger and Krasnow, 1999; Affolter et al., 2003). Beginning with the classic experiments of Alescio and Cassini (Alescio and Cassini, 1962), who demonstrated that lung mesenchyme was sufficient to induce supernumerary buds along the otherwise non-budding tracheal epithelium, work over the last few decades has identified several soluble signals secreted by the mesenchyme that direct the formation and outgrowth of incipient

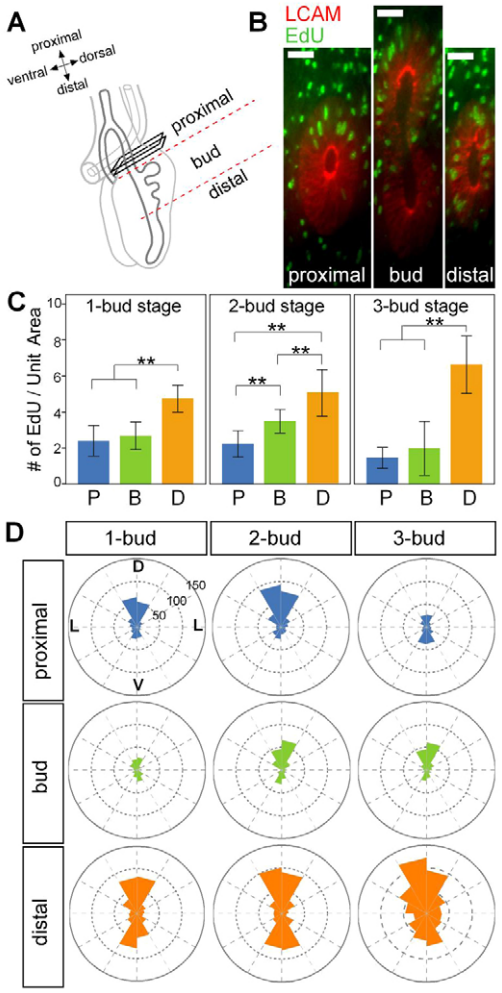

Fig. 5. Spatial patterning of proliferation in the branching airway epithelium. (**A**) Schematic indicating regions (proximal, bud and distal) chosen for quantitative analysis of proliferation. (**B**) Representative cross-sections of a 2-bud-stage lung stained for LCAM and EdU. Scale bars: 100 μm. (**C**) Number of proliferating cells along the primary bronchus at the 1-bud, 2-bud and 3-bud stage. P, proximal; B, bud; D, distal. Unit area=400 μm^2, n=3, $^{**}P$<0.01, error bars represent s.d. (**D**) Circular histogram depicting the angular distribution of proliferating cells with respect to the dorsoventral and lateral axes of the lung. D, dorsal; L, lateral; V, ventral.

buds (Warburton et al., 2000; Morrisey and Hogan, 2010; Ornitz and Yin, 2012). Still, the underlying cellular mechanisms that drive the folding and elongation of the airway epithelium remain unclear. Here, using a combination of theory and experiment, we identified some of the physical and cellular mechanisms that drive monopodial budding of the embryonic chicken lung. Specifically, we found that apical constriction is required to initiate the emergence of new buds from the primary bronchus. Nonetheless, the forces of apical constriction, even when combined with those generated by epithelial cell proliferation, were ultimately insufficient to fully shape the emerging lung bud.

Apical constriction: a conserved physical mechanism for morphogenesis

During embryonic development, simple epithelial sheets bend and fold into a diverse array of tubular structures to accommodate the functions of different organs. Shaping these epithelial tissues requires the generation of forces transmitted between neighboring cells through intercellular polymers and molecular motors (Gorfinkiel and Blanchard, 2011; Kim and Davidson, 2011). The physical mechanisms that transmit and generate these forces include active changes in cell shape (often driven by apical actomyosin contractions) (Haigo et al., 2003; Dawes-Hoang et al., 2005), the addition or deletion of cells via division or apoptosis (Gong et al., 2004; Baena-López et al., 2005; Toyama et al., 2008; Tang et al., 2011), and passive stretching of the tissue in response to either intrinsic or extrinsic forces (Coulombre, 1956; Takeuchi, 1983; Unbekandt et al., 2008).

Apical constriction is an active narrowing of cellular apices that is driven by a contractile actomyosin network, and these changes in cell shape can induce dramatic deformations of the tissue (Sawyer et al., 2010). Many developmental processes involve apical constriction (Taber, 1995; Lecuit and Lenne, 2007; Wozniak and Chen, 2009), including the invagination of epithelial pits, grooves and folds during gastrulation (Martin et al., 2009), neurulation (Colas and Schoenwolf, 2001) and optic cup formation (Plageman et al., 2010). Primary invagination of the *Drosophila* salivary gland and trachea are also driven by apical constriction (Myat and Andrew, 2000b; Letizia et al., 2011).

It is therefore not entirely surprising that apical constriction is involved in the initiation of monopodial branching of the avian airway, in which the epithelial tube folds to produce a bud along its length. We found a dramatic apical shrinkage during the budding process (20% of basal surface), which appears to be similar in magnitude to that measured during invagination of the vertebrate lens placode (36% of basal surface), a process that requires apical localization of actin-binding proteins (Plageman et al., 2010). These numbers are congruent with those measured for apical constriction during *Drosophila* gastrulation, in which the area of the apical surface of initially columnar cells decreases to ~40% of its original value, but with a simultaneous lengthening of the cells (Gelbart et al., 2012). The mechanics of monopodial budding also appear to be distinct from ascidian gastrulation, as invagination of the endoderm involves a substantial cell shortening along the apico-basal axis (Sherrard et al., 2010), which stands in contrast to our observations. Whether these various apical constriction events involve the same underlying regulatory mechanisms remains unclear.

The observation that the FGF receptor inhibitor SU5402 blocked apical constriction and new bud formation in cultured chicken lung explants suggests that sustained apical actomyosin contraction occurs downstream of FGF signaling. Similar to lung development in mice (Bellusci et al., 1997; Park et al., 1998), FGF10 is expressed focally in the embryonic chicken lung in regions of mesenchyme adjacent to emerging buds (Sakiyama et al., 2003; Moura et al., 2011). A feedback mechanism between FGF10 and the transcription factors Tbx4 in the mesenchyme and Nkx2.1 in the epithelium has been shown to regulate monopodial branching in the developing chicken lung (Sakiyama et al., 2003). This pathway might play a role in the apical location of actomyosin structures or in the contractile activity of myosin.

Patterns of apical constriction suggest a more complex regulatory mechanism

Surprisingly, we found that F-actin and pMLC accumulated not only within the dorsal bud-forming region of the primary bronchus, but also along the opposite ventral side of the tube. Moreover, our simulations revealed that apical constriction of both the dorsal and ventral sides of the tube, as well as the tissue stiffening that is likely to result from this constriction, are required to form the leminiscate

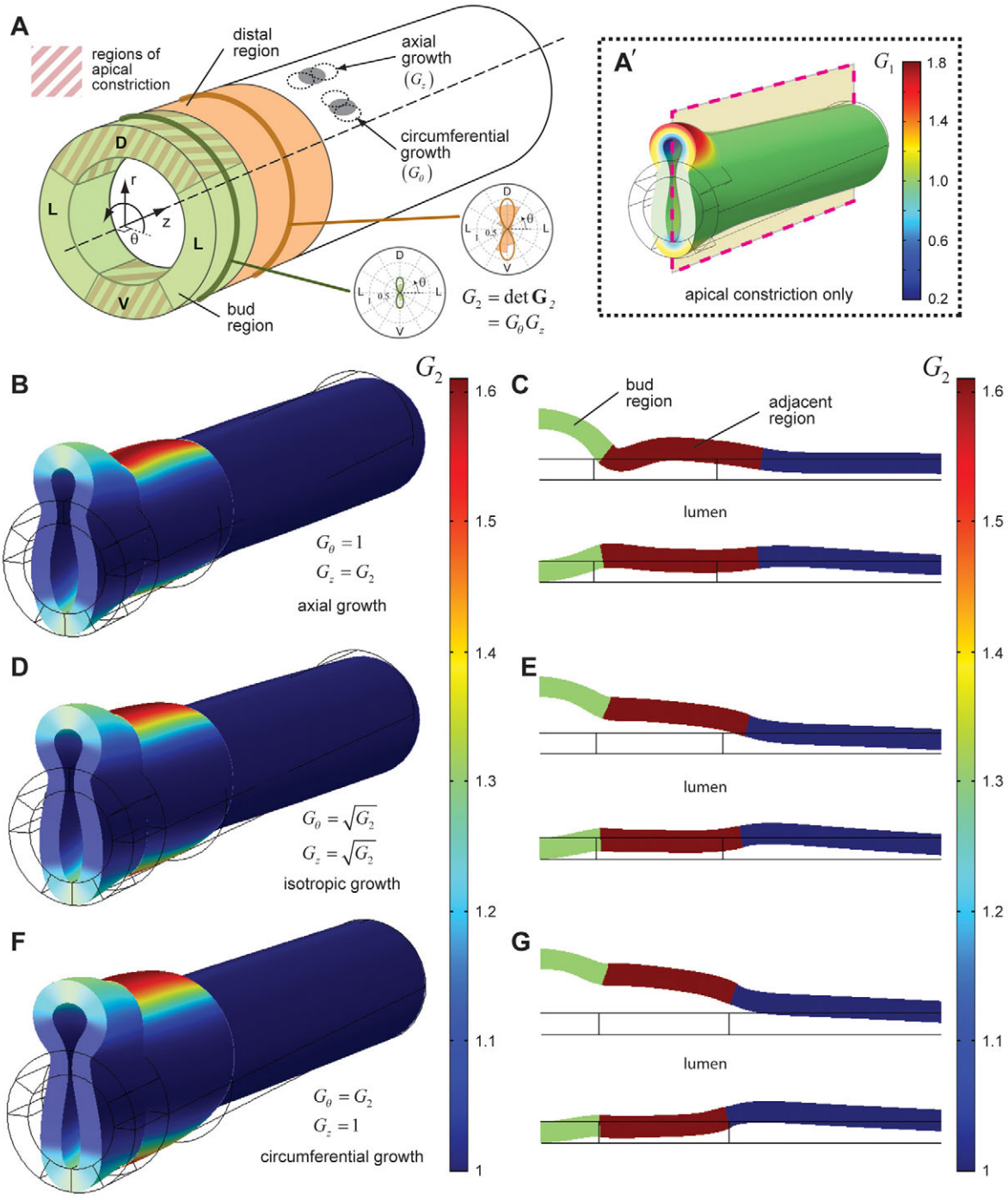

Fig. 6. Cell proliferation and apical constriction together are insufficient to fully shape the early lung bud. (**A**) Model schematic. Cell proliferation was included in both the bud-forming region of the model (green), as well as in an adjacent region of the epithelium (orange). The amount of proliferation in the model was specified by the growth tensor $\mathbf{G}_2$. This growth varied spatially and was consistent with the EdU staining of lungs containing one bud (see Fig. 5C). The overall magnitude of proliferation was specified by $G_2 = \det\mathbf{G}_2 = G_\theta G_z$. For different models, this growth was oriented axially, longitudinally or isotropically – in each case holding G_2 constant. D, dorsal; L, lateral; V, ventral. (**A′**) This growth was superimposed on the pattern of apical constriction specified by G_1 (see Fig. 3). (**B-G**) 3D deformed shape and longitudinal sections (dashed line in A′) for the cases of axial growth (B,C), isotropic growth (D,E) and circumferential growth (F,G). Surface plots represent G_2.

cross-sectional geometry of the bud. These results complicate the generally accepted view that local epithelial-mesenchymal interactions in the bud-forming region alone drive branching morphogenesis, as forces generated by adjacent regions of the tissue contribute physically to this process. The molecular signals that regulate the ventral apical constriction, however, remain unclear; it will be interesting to determine whether these are distinct from the mesenchymal signals that induce apical constriction of the dorsal side, and whether a similar dorsoventral constriction drives domain branching in mammalian lungs.

Monopodial branching is not driven by differential cell proliferation

The addition of cells through proliferation is thought to regulate many morphogenetic movements, including branching of the lung (Nogawa et al., 1998; Tang et al., 2011), and descriptions of the branching process typically suggest that bud outgrowth results from increased proliferation in bud-forming regions (Goldin et al., 1984; Nogawa et al., 1998; Menshykau et al., 2012). Surprisingly, we found that proliferation is neither necessary nor sufficient for bud initiation. That buds can initiate in the absence of proliferation supports the idea that localized changes in cell and tissue shape (in part due to apical constriction) drive the initial stages of monopodial budding, which is similar to the mechanism underlying salivary branching in *Drosophila* (Myat and Andrew, 2000a; Myat and Andrew, 2000b). Consistently, elevated NFκB activity in embryonic chicken lung explants increases the number of buds, yet simultaneously represses proliferation in both the epithelium and mesenchyme (Muraoka et al., 2000). Combined with our results, this provides compelling evidence that proliferation is unnecessary for initiation of monopodial budding of the avian lung.

Nonetheless, our quantitative analysis of EdU-positive cells revealed distinct patterns of cell proliferation within the airway epithelium of the primary bronchus, including elevated proliferation prior to budding and a dorsoventral concentration of proliferation, suggesting that proliferation might contribute to later stages of the branching process. Moreover, differential cell proliferation in the epithelium was observed before the initiation of new buds, as cells distal to emerging buds divided at a higher rate. This stands in contrast to the observations of Nogawa and colleagues, who noted that differential cell proliferation appeared only after the bud had formed in mesenchyme-free embryonic mouse lung explants (Nogawa et al., 1998). This may suggest species-specific differences in monopodial branching, or perhaps even a difference between lungs cultured in mesenchyme-free assays and those that form in the intact embryo.

Our modeling results further demonstrated that differential cell proliferation by itself was insufficient to form a lung bud. Nonetheless, our simulations suggested that proliferation (or some other kind of active elongation in the tissue, e.g. anisotropic changes in cell shape), although not sufficient for bud formation, may still contribute physically to this process, but only if this growth is oriented along the axis of the tube and occurs both within and adjacent to the developing bud. This result is consistent with recently reported evidence of oriented cell divisions driving branch elongation in the developing mouse lung (Tang et al., 2011) and, moreover, suggests that physical forces outside the bud-forming regions play a mechanistic role in this process. Quantitative analysis of the cell division axis within the distal epithelium supports these predictions (supplementary material Fig. S7). Surprisingly, this same analysis revealed that although the dorsal epithelium of the bud does not substantially increase in thickness during monopodial branching (Fig. 2F), a large number of cells within this region preferentially divide perpendicular to the plane of the bud (supplementary material Fig. S7). Such perpendicular cell divisions have been postulated to drive bud extension during dichotomous branching of the mouse lung (Schnatwinkel and Niswander, 2013). Given that the epithelium does not thicken during monopodial branching in the chicken, it is more likely that the cells intercalate within the plane of the bud after cytokinesis. Future quantitative imaging studies are needed to decipher the commonalities and differences between monopodial and dichotomous branching across species.

The inability of both apical constriction and proliferation to generate the fully developed geometry of the bud also suggests a possible physical role for the mesenchyme, as has been suggested for the developing mouse lung (Blanc et al., 2012). Combining experimental and computational studies in the future may help to parse the relative roles of cytoskeletal contractility, oriented cell proliferation, and differential mechanical properties of the epithelium and mesenchyme during airway branching morphogenesis.

Acknowledgements

We thank the members of the Nelson group for their insightful comments.

Funding

This work was supported in part by grants from the National Institutes of Health (NIH) [GM083997 and HL110335]; the David and Lucile Packard Foundation; the Alfred P. Sloan Foundation; the Camille and Henry Dreyfus Foundation; and Susan G. Komen for the Cure. C.M.N. holds a Career Award at the Scientific Interface from the Burroughs Wellcome Fund. Deposited in PMC for release after 12 months.

Competing interests statement

The authors declare no competing financial interests.

Author contributions

H.Y.K., V.D.V. and C.M.N. designed the study. H.Y.K. completed experiments and quantitative imaging. V.D.V. developed the computational model and analyzed results. H.Y.K., V.D.V. and C.M.N. interpreted data and wrote the manuscript.

Supplementary material

Supplementary material available online at
http://dev.biologists.org/lookup/suppl/doi:10.1242/dev.093682/-/DC1

References

Abler, L. L., Mansour, S. L. and Sun, X. (2009). Conditional gene inactivation reveals roles for Fgf10 and Fgfr2 in establishing a normal pattern of epithelial branching in the mouse lung. *Dev. Dyn.* **238**, 1999-2013.

Affolter, M., Bellusci, S., Itoh, N., Shilo, B., Thiery, J.-P. and Werb, Z. (2003). Tube or not tube: remodeling epithelial tissues by branching morphogenesis. *Dev. Cell* **4**, 11-18.

Alescio, T. and Cassini, A. (1962). Induction in vitro of tracheal buds by pulmonary mesenchyme grafted on tracheal epithelium. *J. Exp. Zool.* **150**, 83-94.

Baena-López, L. A., Baonza, A. and García-Bellido, A. (2005). The orientation of cell divisions determines the shape of Drosophila organs. *Curr. Biol.* **15**, 1640-1644.

Bellusci, S., Grindley, J., Emoto, H., Itoh, N. and Hogan, B. L. (1997). Fibroblast growth factor 10 (FGF10) and branching morphogenesis in the embryonic mouse lung. *Development* **124**, 4867-4878.

Blanc, P., Coste, K., Pouchin, P., Azaïs, J.-M., Blanchon, L., Gallot, D. and Sapin, V. (2012). A role for mesenchyme dynamics in mouse lung branching morphogenesis. *PLoS ONE* **7**, e41643.

Caussinus, E., Colombelli, J. and Affolter, M. (2008). Tip-cell migration controls stalk-cell intercalation during Drosophila tracheal tube elongation. *Curr. Biol.* **18**, 1727-1734.

Colas, J.-F. and Schoenwolf, G. C. (2001). Towards a cellular and molecular understanding of neurulation. *Dev. Dyn.* **221**, 117-145.

Coulombre, A. J. (1956). The role of intraocular pressure in the development of the chick eye. I. Control of eye size. *J. Exp. Zool.* **133**, 211-225.

Davies, J. A. (2002). Do different branching epithelia use a conserved developmental mechanism? *Bioessays* **24**, 937-948.

Dawes-Hoang, R. E., Parmar, K. M., Christiansen, A. E., Phelps, C. B., Brand, A. H. and Wieschaus, E. F. (2005). folded gastrulation, cell shape change and the control of myosin localization. *Development* **132**, 4165-4178.

Gelbart, M. A., He, B., Martin, A. C., Thiberge, S. Y., Wieschaus, E. F. and Kaschube, M. (2012). Volume conservation principle involved in cell lengthening and nucleus movement during tissue morphogenesis. *Proc. Natl. Acad. Sci. USA* **109**, 19298-19303.

Gjorevski, N. and Nelson, C. M. (2010). Endogenous patterns of mechanical stress are required for branching morphogenesis. *Integr. Biol. (Camb)* **2**, 424-434.

Gleghorn, J. P., Kwak, J., Pavlovich, A. L. and Nelson, C. M. (2012). Inhibitory morphogens and monopodial branching of the embryonic chicken lung. *Dev. Dyn.* **241**, 852-862.

Goldin, G. V. and Opperman, L. A. (1980). Induction of supernumerary tracheal buds and the stimulation of DNA synthesis in the embryonic chick lung and trachea by epidermal growth factor. *J. Embryol. Exp. Morphol.* **60**, 235-243.

Goldin, G. V. and Wessells, N. K. (1979). Mammalian lung development: the possible role of cell proliferation in the formation of supernumerary tracheal buds and in branching morphogenesis. *J. Exp. Zool.* **208**, 337-346.

Goldin, G. V., Hindman, H. M. and Wessells, N. K. (1984). The role of cell proliferation and cellular shape change in branching morphogenesis of the embryonic mouse lung: analysis using aphidicolin and cytochalasins. *J. Exp. Zool.* **232**, 287-296.
Gong, Y., Mo, C. and Fraser, S. E. (2004). Planar cell polarity signalling controls cell division orientation during zebrafish gastrulation. *Nature* **430**, 689-693.
Gorfinkiel, N. and Blanchard, G. B. (2011). Dynamics of actomyosin contractile activity during epithelial morphogenesis. *Curr. Opin. Cell Biol.* **23**, 531-539.
Haigo, S. L., Hildebrand, J. D., Harland, R. M. and Wallingford, J. B. (2003). Shroom induces apical constriction and is required for hingepoint formation during neural tube closure. *Curr. Biol.* **13**, 2125-2137.
Harding, M. J. and Nechiporuk, A. V. (2012). Fgfr-Ras-MAPK signaling is required for apical constriction via apical positioning of Rho-associated kinase during mechanosensory organ formation. *Development* **139**, 3130-3135.
Hogan, B. L. M. (1999). Morphogenesis. *Cell* **96**, 225-233.
Kim, H. Y. and Davidson, L. A. (2011). Punctuated actin contractions during convergent extension and their permissive regulation by the non-canonical Wnt-signaling pathway. *J. Cell Sci.* **124**, 635-646.
Kovács, M., Tóth, J., Hetényi, C., Málnási-Csizmadia, A. and Sellers, J. R. (2004). Mechanism of blebbistatin inhibition of myosin II. *J. Biol. Chem.* **279**, 35557-35563.
Lecuit, T. and Lenne, P.-F. (2007). Cell surface mechanics and the control of cell shape, tissue patterns and morphogenesis. *Nat. Rev. Mol. Cell Biol.* **8**, 633-644.
Letizia, A., Sotillos, S., Campuzano, S. and Llimargas, M. (2011). Regulated Crb accumulation controls apical constriction and invagination in Drosophila tracheal cells. *J. Cell Sci.* **124**, 240-251.
Locy, W. A. and Larsell, O. (1916). The embryology of the bird's lung. Based on observations of the domestic fowl. Part 1. *Am. J. Anat.* **19**, 447-504.
Martin, A. C., Kaschube, M. and Wieschaus, E. F. (2009). Pulsed contractions of an actin-myosin network drive apical constriction. *Nature* **457**, 495-499.
Menshykau, D., Kraemer, C. and Iber, D. (2012). Branch mode selection during early lung development. *PLOS Comput. Biol.* **8**, e1002377.
Metzger, R. J. and Krasnow, M. A. (1999). Genetic control of branching morphogenesis. *Science* **284**, 1635-1639.
Metzger, R. J., Klein, O. D., Martin, G. R. and Krasnow, M. A. (2008). The branching programme of mouse lung development. *Nature* **453**, 745-750.
Michael, L. and Davies, J. A. (2004). Pattern and regulation of cell proliferation during murine ureteric bud development. *J. Anat.* **204**, 241-255.
Michael, L., Sweeney, D. E. and Davies, J. A. (2005). A role for microfilament-based contraction in branching morphogenesis of the ureteric bud. *Kidney Int.* **68**, 2010-2018.
Miura, T., Hartmann, D., Kinboshi, M., Komada, M., Ishibashi, M. and Shiota, K. (2009). The cyst-branch difference in developing chick lung results from a different morphogen diffusion coefficient. *Mech. Dev.* **126**, 160-172.
Moore, K. A., Huang, S., Kong, Y., Sunday, M. E. and Ingber, D. E. (2002). Control of embryonic lung branching morphogenesis by the Rho activator, cytotoxic necrotizing factor 1. *J. Surg. Res.* **104**, 95-100.
Moore, K. A., Polte, T., Huang, S., Shi, B., Alsberg, E., Sunday, M. E. and Ingber, D. E. (2005). Control of basement membrane remodeling and epithelial branching morphogenesis in embryonic lung by Rho and cytoskeletal tension. *Dev. Dyn.* **232**, 268-281.
Morrisey, E. E. and Hogan, B. L. M. (2010). Preparing for the first breath: genetic and cellular mechanisms in lung development. *Dev. Cell* **18**, 8-23.
Moura, R. S., Coutinho-Borges, J. P., Pacheco, A. P., Damota, P. O. and Correia-Pinto, J. (2011). FGF signaling pathway in the developing chick lung: expression and inhibition studies. *PLoS ONE* **6**, e17660.
Muñoz, J. J., Barrett, K. and Miodownik, M. (2007). A deformation gradient decomposition method for the analysis of the mechanics of morphogenesis. *J. Biomech.* **40**, 1372-1380.
Muñoz, J. J., Conte, V. and Miodownik, M. (2010). Stress-dependent morphogenesis: continuum mechanics and truss systems. *Biomech. Model. Mechanobiol.* **9**, 451-467.
Muraoka, R. S., Bushdid, P. B., Brantley, D. M., Yull, F. E. and Kerr, L. D. (2000). Mesenchymal expression of nuclear factor-kappaB inhibits epithelial growth and branching in the embryonic chick lung. *Dev. Biol.* **225**, 322-338.
Myat, M. M. and Andrew, D. J. (2000a). Fork head prevents apoptosis and promotes cell shape change during formation of the Drosophila salivary glands. *Development* **127**, 4217-4226.
Myat, M. M. and Andrew, D. J. (2000b). Organ shape in the Drosophila salivary gland is controlled by regulated, sequential internalization of the primordia. *Development* **127**, 679-691.
Nakanishi, Y., Morita, T. and Nogawa, H. (1987). Cell proliferation is not required for the initiation of early cleft formation in mouse embryonic submandibular epithelium in vitro. *Development* **99**, 429-437.
Nelson, C. M. and Gleghorn, J. P. (2012). Sculpting organs: mechanical regulation of tissue development. *Annu. Rev. Biomed. Eng.* **14**, 129-154.
Nogawa, H., Morita, K. and Cardoso, W. V. (1998). Bud formation precedes the appearance of differential cell proliferation during branching morphogenesis of mouse lung epithelium in vitro. *Dev. Dyn.* **213**, 228-235.
Ornitz, D. M. and Yin, Y. (2012). Signaling networks regulating development of the lower respiratory tract. *Cold Spring Harb. Perspect. Biol.* **4**, a008318.
Park, W. Y., Miranda, B., Lebeche, D., Hashimoto, G. and Cardoso, W. V. (1998). FGF-10 is a chemotactic factor for distal epithelial buds during lung development. *Dev. Biol.* **201**, 125-134.
Plageman, T. F., Jr, Chung, M.-I., Lou, M., Smith, A. N., Hildebrand, J. D., Wallingford, J. B. and Lang, R. A. (2010). Pax6-dependent Shroom3 expression regulates apical constriction during lens placode invagination. *Development* **137**, 405-415.
Rémond, M. C., Fee, J. A., Elson, E. L. and Taber, L. A. (2006). Myosin-based contraction is not necessary for cardiac c-looping in the chick embryo. *Anat. Embryol. (Berl.)* **211**, 443-454.
Rodriguez, E. K., Hoger, A. and McCulloch, A. D. (1994). Stress-dependent finite growth in soft elastic tissues. *J. Biomech.* **27**, 455-467.
Sai, X. and Ladher, R. K. (2008). FGF signaling regulates cytoskeletal remodeling during epithelial morphogenesis. *Curr. Biol.* **18**, 976-981.
Sakiyama, J.-i., Yamagishi, A. and Kuroiwa, A. (2003). Tbx4-Fgf10 system controls lung bud formation during chicken embryonic development. *Development* **130**, 1225-1234.
Sawyer, J. M., Harrell, J. R., Shemer, G., Sullivan-Brown, J., Roh-Johnson, M. and Goldstein, B. (2010). Apical constriction: a cell shape change that can drive morphogenesis. *Dev. Biol.* **341**, 5-19.
Schnatwinkel, C. and Niswander, L. (2013). Multiparametric image analysis of lung-branching morphogenesis. *Dev. Dyn.*
Schneider, C. A., Rasband, W. S. and Eliceiri, K. W. (2012). NIH Image to ImageJ: 25 years of image analysis. *Nat. Methods* **9**, 671-675.
Sherrard, K., Robin, F., Lemaire, P. and Munro, E. (2010). Sequential activation of apical and basolateral contractility drives ascidian endoderm invagination. *Curr. Biol.* **20**, 1499-1510.
Spooner, B. S., Bassett, K. E. and Spooner, B. S., Jr (1989). Embryonic salivary gland epithelial branching activity is experimentally independent of epithelial expansion activity. *Dev. Biol.* **133**, 569-575.
Straight, A. F., Cheung, A., Limouze, J., Chen, I., Westwood, N. J., Sellers, J. R. and Mitchison, T. J. (2003). Dissecting temporal and spatial control of cytokinesis with a myosin II Inhibitor. *Science* **299**, 1743-1747.
Taber, L. A. (1995). Biomechanics of growth, remodeling, and morphogenesis. *Appl. Mech. Rev.* **48**, 487-545.
Taber, L. A. (2004) *Nonlinear Theory of Elasticity: Applications in Biomechanics*. Singapore: World Scientific.
Taber, L. A. (2008). Theoretical study of Beloussov's hyper-restoration hypothesis for mechanical regulation of morphogenesis. *Biomech. Model. Mechanobiol.* **7**, 427-441.
Takeuchi, S. (1983). Wound healing in the cornea of the chick embryo. V. An observation and quantitative assessment of the cell shapes in the isolated corneal epithelium during spreading in vitro. *Cell Tissue Res.* **229**, 109-127.
Tang, N., Marshall, W. F., McMahon, M., Metzger, R. J. and Martin, G. R. (2011). Control of mitotic spindle angle by the RAS-regulated ERK1/2 pathway determines lung tube shape. *Science* **333**, 342-345.
Toyama, Y., Peralta, X. G., Wells, A. R., Kiehart, D. P. and Edwards, G. S. (2008). Apoptotic force and tissue dynamics during Drosophila embryogenesis. *Science* **321**, 1683-1686.
Unbekandt, M., del Moral, P.-M., Sala, F. G., Bellusci, S., Warburton, D. and Fleury, V. (2008). Tracheal occlusion increases the rate of epithelial branching of embryonic mouse lung via the FGF10-FGFR2b-Sprouty2 pathway. *Mech. Dev.* **125**, 314-324.
Varner, V. D. and Taber, L. A. (2012). Not just inductive: a crucial mechanical role for the endoderm during heart tube assembly. *Development* **139**, 1680-1690.
Varner, V. D., Voronov, D. A. and Taber, L. A. (2010). Mechanics of head fold formation: investigating tissue-level forces during early development. *Development* **137**, 3801-3811.
Voronov, D. A., Alford, P. W., Xu, G. and Taber, L. A. (2004). The role of mechanical forces in dextral rotation during cardiac looping in the chick embryo. *Dev. Biol.* **272**, 339-350.
Wakatsuki, T., Kolodney, M. S., Zahalak, G. I. and Elson, E. L. (2000). Cell mechanics studied by a reconstituted model tissue. *Biophys. J.* **79**, 2353-2368.
Wakatsuki, T., Schwab, B., Thompson, N. C. and Elson, E. L. (2001). Effects of cytochalasin D and latrunculin B on mechanical properties of cells. *J. Cell Sci.* **114**, 1025-1036.
Warburton, D., Schwarz, M., Tefft, D., Flores-Delgado, G., Anderson, K. D. and Cardoso, W. V. (2000). The molecular basis of lung morphogenesis. *Mech. Dev.* **92**, 55-81.
Wessells, N. K. (1970). Mammalian lung development: interactions in formation and morphogenesis of tracheal buds. *J. Exp. Zool.* **175**, 455-466.
Wozniak, M. A. and Chen, C. S. (2009). Mechanotransduction in development: a growing role for contractility. *Nat. Rev. Mol. Cell Biol.* **10**, 34-43.
Zhou, J., Kim, H. Y. and Davidson, L. A. (2009). Actomyosin stiffens the vertebrate embryo during crucial stages of elongation and neural tube closure. *Development* **136**, 677-688.